Journal of Power Sources 344 (2017) 11–14

Contents lists available at ScienceDirect

Journal of Power Sources

journal homepage: www.elsevier.com/locate/jpowsour

Design, synthesis and application of a π-conjugated, non-spiro molecular alternative as hole-transport material for highly efficient dye-sensitized solar cells and perovskite solar cells

Peng Liu [a, 1], Bo Xu [b, 1], Yong Hua [a, 1], Ming Cheng [b], Kerttu Aitola [c], Kári Sveinbjörnsson [c], Jinbao Zhang [c], Gerrit Boschloo [c], Licheng Sun [b, **], Lars Kloo [a, *]

[a] Applied Physical Chemistry, Center of Molecular Devices, Department of Chemistry, School of Chemical Science and Engineering, KTH-Royal Institute of Technology, SE-10044 Stockholm, Sweden
[b] Organic Chemistry, Center of Molecular Devices, Department of Chemistry, School of Chemical Science and Engineering, KTH-Royal Institute of Technology, SE-10044 Stockholm, Sweden
[c] Department of Chemistry-Ångstrom Laboratory, Physical Chemistry, Uppsala University, SE-75120 Uppsala, Sweden

HIGHLIGHTS

- Two small, π-conjugated HTMs were synthesized for efficient ssDSSCs and PSCs.
- The novel HTM **X14** shows the highest PCEs of 6.1% for ssDSSCs and 16.4% for PSCs.
- PIA and PL results show efficient charge transfer at the materials interfaces.
- Enhancement of molecular π-conjugation improves conductivity.

ARTICLE INFO

Article history:
Received 28 November 2016
Received in revised form
18 January 2017
Accepted 21 January 2017
Available online 29 January 2017

Keywords:
Hole-transport materials
Dye-sensitized solar cells
Perovskite solar cells

ABSTRACT

Two low-cost, easily synthesized π-conjugated molecules have been applied as hole-transport materials (HTMs) for solid state dye-sensitized solar cells (ssDSSCs) and perovskite solar cells (PSCs). For X1-based devices, high power conversion efficiencies (PCEs) of 5.8% and 14.4% in ssDSSCs and PSCs has been demonstrated. For X14-based devices, PCEs were improved to 6.1% and 16.4% in ssDSCs and PSCs, respectively.

1. Introduction

For decades, scientists have been dedicated to exploring new clean and renewable energy sources. Among those, solution-processable photovoltaic devices, such as solid state dye-sensitized solar cells (ssDSSCs) [1] and perovskite solar cells (PSCs) [2,3] have attracted much attention due to their potential low cost in large-scale production together with high PCEs. In such devices, hole transport materials (HTM) have been shown to play a crucial role in achieving the high performance. The main function of the HTMs in the ssDSSCs and PSCs is to scavenge photo-generated holes in the light-harvesting materials and subsequently transport the holes to the counter electrodes. In the research area of DSSCs, solid-state HTMs have been developed to replace the liquid electrolyte [1,4–7]. In 2011, ssDSSCs with an excellent 7.2% efficiency was reported by Grätzel and co-workers, and those cells were based on the HTM 2,2′,7-,7′-tetrakis(N,N-di-*p*-methoxyphenylamine) 9,9′-spirobifuorene (Spiro-OMeTAD) employing a cobalt-complex dopant and custom-synthesized dyes [8]. Since this work, the Spiro-OMeTAD HTM has become the champion material to beat. Recently, PSCs showing >15% power conversion efficiency have boosted the research field both

* Corresponding author.
** Corresponding author.
E-mail addresses: Lichengs@kth.se (L. Sun), Lakloo@kth.se (L. Kloo).
[1] These authors have contributed equally.

http://dx.doi.org/10.1016/j.jpowsour.2017.01.092

concerning the number of active scientists and new materials published [3,9,10].

Spiro-OMeTAD, because of its good solubility in commonly used organic solvents and accessibility (in spite of its high cost), has become the 'standard' HTM in ssDSSCs [8,11,12] and PSCs. However, due to the disadvantage of high cost, low conductivity and relatively poor ability to infiltrate a mesoporous substrate, much effort has been made to identify alternatives [13–17]. Kim and his coworkers introduced in situ solid state polymerization of conducting polymers for highly efficient ssDSSCs [18]. Xu, Tian, Hagfeldt and Sun developed a triphenylamine-based oligomer hole-transport material introduced into ssDSSCs and obtained 5.8% conversion efficiency [19], and they lately improved the efficiency up to 6.0% by using carbazole-based HTMs [20]. Recently, A low-cost spiro[fluorene-9,9′-xanthene] (SFX) based organic hole-transport material (HTM), termed **X60**, was applied in ssDSSCs and PSCs with efficiencies of 7.3% and 19.8%, respectively [21]. Yong Hua et al. designed fluorine-based HTMs and achieved an efficiency of 6.4% in ssDSSCs and 18.0% in PSCs using the material **HT2** as the HTM [22]. Recently, Jinbao Zhang et al. studied the effect of alkyl chains on organic HTMs for efficient perovskite solar cells reporting efficiencies up to 17.3% [23]. In addition, Lei, Xu, Sun, Hagfeldt and coworkers used a small-molecule, hole-transport material (**MeO-TPD, X1**) to obtain 4.8% conversion efficiency [24] in ssDSSCs. In this work, we report HTMs based on small molecules characterized by a higher degree of π-conjugation; viz. **X14 (N4,N4,N4′,N4'-tetrakis(2′,4'-dimethoxy-[1,1'-biphenyl]-4-yl)-[1,1'-biphenyl]-4,4'-diamine)**, compared with the already known **X1**, and applied to ssDSSCs and PSCs. In comparison with Spiro-OMeTAD, the synthesis route for X14 is much more straightforward and facile. Therefore, the cost of devices would be reduced significantly. More details can be found in the Supporting Information. The molecular structures of the materials studied in this work are presented in Fig. 1.

2. Results and discussion

Quantum chemical calculations (see the Supporting Information)were performed to estimate the electronic and optical properties of the HTMs studied in this work. As shown in Fig. 1b, in the case of **X1**, the highest occupied molecular orbital (HOMO) is delocalized throughout the entire molecule, while the lowest unoccupied molecular orbital (LUMO) is mainly localized on the central biphenyl part. In contrast, both the HOMO and LUMO orbitals in **X14** are delocalized over the whole molecule, which can be attributed to the enhanced π-conjugation effect. The HOMO and LUMO orbitals overlap in the X14 molecules indication the formation of neutral excitons and hole-transfer transition, due to the strong Coulomb interaction [22]. It was also noted that calculated trends of HOMO energy levels, as well as ionization potentials, agree well with experimental data. More details can be found in the Supporting Information. The calculated singlet excitation energies using time-dependent density-functional theory (TDDFT) are summarized in Table 1. In addition, the re-organization energy is an important factor influencing the hole-transport efficiency. Here, we calculated the re-organization energy of the HTMs used in this work followed our previous paper (Table 1) [7]. In comparison with **X1**, **X14** shows a lower reorganization energy by 176 meV, indicating the highest hole mobility among the HTMs. We also determined the conductivity of the HTMs under different conditions (Table 2). For both non-doped and doped materials, **X14** comes out with the best conductivity properties, which is in good agreement with our theoretical studies.

The UV–Vis absorption spectra of **X1** and **X14** are shown in

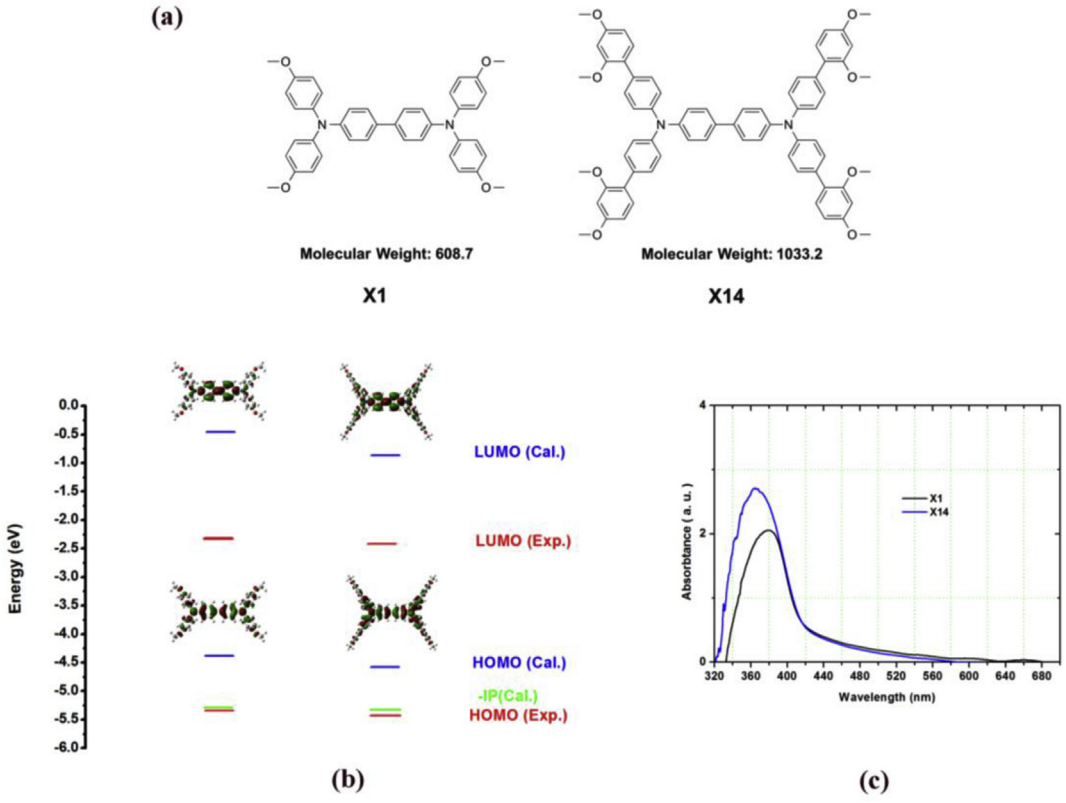

Fig. 1. (a) molecular structure of X1 and X14, (b) Energy alignment (vs. vacuum) and (c) UV–vis absorption.

Table 1
Summary of the calculated and experimental HTM optical and electronic properties.

	Calculated data				Experimental data				
	HOMO (eV)	LUMO (eV)	-IP[a] (eV)	E_g[b] (eV)	λ_{hole} (meV)	λ_{max} (nm)	E_{optgap}[c] (eV)	LUMO[d] (eV)	HOMO (eV)
X1	−4.32	−0.46	−5.22	3.82	208	380	2.96	−2.35	−5.31
X14	−4.54	−0.87	−5.28	3.68	176	364	2.92	−2.45	−5.37

[a] Ionization potential (IP) calculated by total energy difference of E_{cation}-$E_{neutral}$.
[b] S_0-S_1 excitation energy determined from TDDFT calculations using the MPW1K/6-31G* level of theory.
[c] Optical band gap determined by the UV−vis absorption onset.
[d] $E_{LUMO} = E_{HOMO} + E_{optgap}$.

Table 2
Hole conductivity of different HTMs (S cm^{-1}).

	Without doping	Li(TFSI) doping	Ag(TFSI) doping
X1	$4.95*10^{-7}$	$1.53*10^{-4}$	$1.78*10^{-4}$
X14	$5.01*10^{-7}$	$3.23*10^{-4}$	$4.01*10^{-4}$

Table 3
Photovoltaic parameters of devices studied at a light intensity of 100 mW cm^2 (AM 1.5G). All HTM solutions used to fabricate the solar cells were doped with 2 mM Ag(TFSI).

	Jsc (mA cm^{-2})	Voc (V)	FF	PEC
ssDSSCs				
X1	9.44	0.88	0.69	5.8%
X14	9.71	0.91	0.71	6.1%
Spiro-OMeTAD	9.41	0.89	0.7	5.9%
PSC				
X1	20.81	1.06	0.65	14.4%
X14	22.59	1.09	0.67	16.4%
Spiro-OMeTAD	22.14	1.08	0.65	15.6%

Fig. 1c. **X1** and **X14** show a single absorption peak centered at 380 and 364 nm, respectively. The spectra of **X14** show a slight blue-shift as compared to **X1**, which can be attributed to in the higher degree of π-conjugation. The optical band gap (E_g) is calculated from the absorption onset wavelength of the corresponding absorption spectrum. Cyclic voltammograms of solutions of **X14** are shown in the Supporting Information. The redox peaks of **X14** are reversible, indicating that the substance has good electrochemical stability. Further, the reported HOMO energy of the dye LEG4 is −5.48 eV [7], which indicates that all the HTMs stadied have energetics favorable for the hole-transfer process. Both energy levels of the HOMO of the HTMs are lower than the HOMO energy level of Spiro-OMeTAD, which may facility higher V_{oc} for the corresponding devices. Table 1 summarizes the optical and electrochemical properties of the two HTMs.

Fig. 2 shows the *J*–*V* curves of the ssDSSCs based on the HTMs **X1** and **X14**, and the corresponding photovoltaic parameters are tabulated in Table 3. For comparison, a reference cell containing well-studied Spiro-OMeTAD HTM was also fabricated using the same fabrication process as for the new HTMs. The **X1** ssDSSCs solar cells provided a J_{sc} of 9.44 mA cm^{-2}, a V_{oc} of 880 mV and an *FF* of 0.69, affording a final PCE of 5.8%. These photovoltaic parameters are comparable to that of the cells based on Sprio-OMeTAD (J_{sc} of 9.41 mA cm^{-2}, V_{oc} of 885 mV, *FF* of 0.7, and PCE of 5.9%). Under the same conditions, the **X14**-based cells showed a J_{sc} of 9.71 mA cm^{-2}, a V_{oc} of 905 mV and an *FF* of 0.71, corresponding to a PCE of 6.1%. The corresponding IPCE spectra show a similar trend for all HTM-based devices agreeing well with the recorded J_{sc}. Clearly, the photovoltaic performance is quite sensitive to structural modifications of the HTM molecular building blocks. Moreover, the higher fill factor noted for devices containing **X14** can most likely be attributed to its higher conductivity. Based on the electron lifetime measurements (see Supporting Information), the devices based on X14 show longer electron lifetime in correspondance with the recorded device V_{oc}. In order to investigate the charge-transfer properties, photoinduced absorption spectra were also recorded. A film of LEG4 on the TiO_2 substrate shows positive values between 650 and 850 nm, which can be assigned to the oxidized state of LEG4 [25]. After hole-transport material deposition, the positive peaks are quenched due to charge transfer at the interface of the dye/HTMs. In the presence of all three HTMs, a significant reduction of the oxidized dye absorption can be observed indicating efficient dye regeneration in the corresponding ssDSSCs. All the curves are quite similar, indicating similar dye regeneration yields. This is also in good agreement with the recorded J_{sc} for the devices. The above results clearly show that **X14** is suitable to be used as an HTM in ssDSSCs.

Fig. 3a shows the current-voltage characteristics for PSCs based on Spiro-OMeTAD, **X1** and **X14**, respectively. The photovoltaic parameters are summarized in Table 3. In addition, the *J-V* curves under the forward and backward scan directions are shown in Table S1 in the Supporting Information, and the corresponding

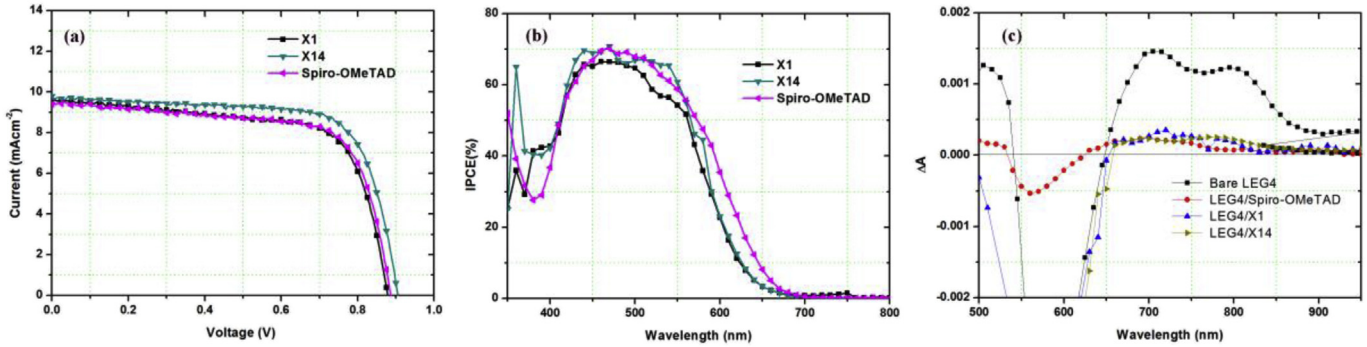

Fig. 2. (a) J-V curve for ssDSSCs (b) IPCE spectra (c) Photo-induced absorption spectra.

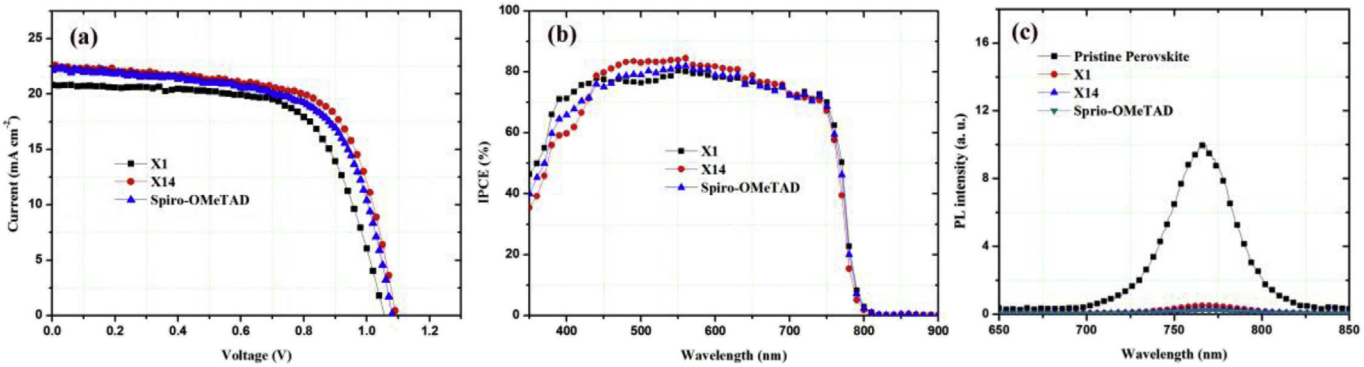

Fig. 3. (a) J-V curve for PSCs (scan from Voc to 0 V, scan rate 40 mV), (b) IPCE spectra and (c) Steady-state photoluminescence spectra of FTO/Al_2O_3/perovskite films based on different HTMs.

photovoltaic parameters are listed in Table S1. The **X1**-based devices display an efficiency of 14.4%, with a J_{sc} of 20.81 mA cm^{-2}, a V_{oc} of 1.06 V, and an *FF* of 0.65. As a reference, Spiro-OMeTAD-based PSCs offer a slightly higher PCE of 15.6%, with a short-circuit density (J_{sc}) of 22.14 mAcm^{-2}, an open-circuit voltage (V_{oc}) of 1.08 V, and a fill factor (FF) of 0.65. Interestingly, the mixed-ion PSCs containing the HTM **X14** render the best photovoltaic performance with a PCE of 16.4% (J_{sc} = 22.14 mA cm^{-2}, V_{oc} = 1.08 V, and *FF* = 0.65). The incident photon-to-current conversion efficiency (IPCE) spectra for the devices containing **X1**, **X14** and Spiro-OMeTAD are shown in Fig. 3b. The **X14**-based devices show the highest IPCEs, which agrees with the excellent J_{sc} recorded for such devices. In addition, the statistical data of PSCs based on the three HTMs are given in Fig. S2. Based on the results of electrochemical impedance spectroscopy (Fig. S8), the devices based on X14 show the highest recombination resistance, resulting in the slowest recombination rate. In order to investigate the charge transfer at the interface between the perovskite and hole-transport materials photoluminescence spectra were recorded and these are shown in Fig. 3c demonstrating that the perovskite film without HTMs shows a strong PL signal due to the recombination between the photogenerated electrons and holes. A dramatic decrease of PL intensity is observed after the deposition of an HTM layers on top of the perovskite layer, especially for the **X14**-based devices. An efficient quenching of the photogenerated charges can lead to fast interface charge separation in **X14**-based devices, contributing to a better J_{sc} and *FF* in the PSCs, as compared to Spiro-OMeTAD-based devices.

3. Conclusion

Two small, π-conjugated hole-transport materials (HTMs) have been designed, synthesized and applied in highly efficient ssDSSCs and PSCs. It was found that the enhancement of molecular π-conjugation significantly may improve both conductivity and charge delocalization in the molecules building the HTMs. The synthesis route for HTMs is much more facile and environmental friendly, compared with Spiro-OMeTAD. The devices based on the HTM **X14** shows the highest PCEs of 6.1% for ssDSSCs and 16.4% for PSCs, which can be traced to the material's fast charge-transport ability and efficient charge-separation properties. This work provides instructive suggestions for the future design of new and even more efficient hole-transport materials for solid state dye-sensitized and perovskite solar cells.

Acknowledgements

The Swedish Research Council, the Swedish Energy Agency and Knut & Alice Wallenberg Foundation are gratefully acknowledged for their financial support.

Appendix A. Supplementary data

Supplementary data related to this article can be found at http://dx.doi.org/10.1016/j.jpowsour.2017.01.092.

References

[1] U. Bach, D. Lupo, P. Comte, J.E. Moser, F. Weissortel, J. Salbeck, H. Spreitzer, M. Gratzel, Nature 395 (1998) 583–585.
[2] M.M. Lee, J. Teuscher, T. Miyasaka, T.N. Murakami, H.J. Snaith, Science 338 (2012) 643–647.
[3] H.-S.S. Kim, C.-R.R. Lee, J.-H.H. Im, K.-B.B. Lee, T. Moehl, A. Marchioro, S.-J.J. Moon, R. Humphry-Baker, J.-H.H. Yum, J.E. Moser, M. Grätzel, N.-G.G. Park, Sci. Rep. 2 (2012) 591.
[4] L. Bin, W. Liduo, K. Bonan, W. Peng, Q. Yong, Sol. Energy Mater. Sol. Cells 90 (2006) 549–573.
[5] N. Cai, S.-J. Moon, L. Cevey-Ha, T. Moehl, R. Humphry-Baker, P. Wang, S.M. Zakeeruddin, M. Grätzel, Nano Lett. 11 (2011) 1452–1456.
[6] P. Liu, J.M. Gardner, L. Kloo, Chem. Commun. 51 (2015) 14660–14662.
[7] P. Liu, B. Xu, K.M. Karlsson, J. Zhang, N. Vlachopoulos, G. Boschloo, L. Sun, L. Kloo, J. Mater. Chem. A 3 (2015) 4420–4427.
[8] J. Burschka, A. Dualeh, F. Kessler, E. Baranoff, N.-L.L. Cevey-Ha, C. Yi, M.K. Nazeeruddin, M. Grätzel, J. Am. Chem. Soc. 133 (2011) 18042–18045.
[9] J. Burschka, N. Pellet, S.-J.J. Moon, R. Humphry-Baker, P. Gao, M.K. Nazeeruddin, M. Grätzel, Nature 499 (2013) 316–319.
[10] N.J. Jeon, J.H. Noh, Y.C. Kim, W.S. Yang, S. Ryu, S.I. Seok, Nat. Mater. (2014) 897–903.
[11] H.J. Snaith, A.J. Moule, C. Klein, K. Meerholz, R.H. Friend, M. Grätzel, Nano Lett. 7 (2007) 3372–3376.
[12] W. Mingkui, X. Mingfei, S. Dong, L. Renzhi, G. Feifei, Z. Guangliang, Y. Zhihui, H.-B. Robin, W. Peng, M.Z. Shaik, G. Michael, Adv. Mater. (2008) 4460–4463.
[13] T. Leijtens, I.K.K. Ding, T. Giovenzana, J.T. Bloking, M.D. McGehee, A. Sellinger, ACS Nano 6 (2012) 1455–1462.
[14] H. Wang, X. Zhang, F. Gong, G. Zhou, Z.-S. Wang, Adv. Mater. 24 (2012) 121–124.
[15] J.E. Kroeze, N. Hirata, L. Schmidt-Mende, C. Orizu, S.D. Ogier, K. Carr, M. Grätzel, J.R. Durrant, Adv. Func. Mater. 16 (2006) 1832–1838.
[16] B.-W. Park, L. Yang, E.M.J. Johansson, N. Vlachopoulos, A. Chams, C. Perruchot, M. Jouini, G. Boschloo, A. Hagfeldt, J. Phys. Chem. C 117 (2013) 22484–22491.
[17] M. Cheng, B. Xu, C. Chen, X. Yang, F. Zhang, Q. Tan, Y. Hua, L. Kloo, L. Sun, Adv. Energy Mater. 5 (2015) n/a-n/a.
[18] J.K. Koh, J. Kim, B. Kim, J.H. Kim, E. Kim, Adv. Mater. 23 (2011) 1641–1646.
[19] B. Xu, H. Tian, D. Bi, E. Gabrielsson, E.M.J. Johansson, G. Boschloo, A. Hagfeldt, L. Sun, J. Mater. Chem. A 1 (2013) 14467–14470.
[20] B. Xu, E. Sheibani, P. Liu, J. Zhang, H. Tian, N. Vlachopoulos, G. Boschloo, L. Kloo, A. Hagfeldt, L. Sun, Adv. Mater. 26 (38) (October 15, 2014) 6629–6634.
[21] B. Xu, D. Bi, Y. Hua, P. Liu, M. Cheng, M. Gratzel, L. Kloo, A. Hagfeldt, L. Sun, Energy Environ. Sci. 9 (2016) 873–877.
[22] Y. Hua, J. Zhang, B. Xu, P. Liu, M. Cheng, L. Kloo, E.M.J. Johansson, K. Sveinbjörnsson, K. Aitola, G. Boschloo, L. Sun, Nano Energy 26 (2016) 108–113.
[23] J. Zhang, B. Xu, M.B. Johansson, M. Hadadian, J.P. Correa Baena, P. Liu, Y. Hua, N. Vlachopoulos, E.M.J. Johansson, G. Boschloo, L. Sun, A. Hagfeldt, Adv. Energy Mater. (2016) 1502536.
[24] L. Yang, B. Xu, D. Bi, H. Tian, G. Boschloo, L. Sun, A. Hagfeldt, E.M. Johansson, J. Am. Chem. Soc. 135 (2013) 7378–7385.
[25] W. Yang, N. Vlachopoulos, Y. Hao, A. Hagfeldt, G. Boschloo, Phys. Chem. Chem. Phys. (2015) 15868–15875.